

Nuclear dissociation after the O 1s →($^4\Sigma_u^-$)3sσ excitation in O2 molecules

Bocheng Ding(丁伯承), Ruichang Wu(吴睿昌), Yunfei Feng(封云飞), and Xiaojing Liu(刘小井)

Citation: Chin. Phys. B, 2022, 31 (**8**): 083301. DOI: 10.1088/1674-1056/ac560b
Journal homepage: http://cpb.iphy.ac.cn; http://iopscience.iop.org/cpb

What follows is a list of articles you may be interested in

Coulomb explosion of CS_2 molecule under an intense femtosecond laser field

Xiao Wang(王潇), Jian Zhang(张健), Shi-An Zhang(张诗按), Zhen-Rong Sun(孙真荣)
Chin. Phys. B, 2016, 25 (**5**): 053301. DOI: 10.1088/1674-1056/25/5/053301

Effect of pump-1 laser on Autler–Townes splitting in photoelectron spectrum of K_2 molecule

Guo Wei, Lu Xing-Qiang, Wang Xin-Lin, Yao Hong-Bin
Chin. Phys. B, 2015, 24 (**1**): 013302. DOI: 10.1088/1674-1056/24/1/013302

Time-dependent approach to the double-channel dissociation of the NaCs molecule induced by pulsed lasers

Zhang Cai-Xia, Niu Yu-Quan, Meng Qing-Tian
Chin. Phys. B, 2014, 23 (**10**): 103301. DOI: 10.1088/1674-1056/23/10/103301

Manifestation of external field effect in time-resolved photo-dissociation dynamics of LiF

Meng Qing-Tian, A. J. C. Varandas
Chin. Phys. B, 2013, 22 (**7**): 073303. DOI: 10.1088/1674-1056/22/7/073303

Laser guiding of cold molecules in a hollow optical fiber and continuous-wave cold molecular beam generation

Liu Run-Qin(刘润琴), Yin Ya-Ling(尹亚玲), and Yin Jian-Ping(印建平)
Chin. Phys. B, 2012, 21 (**3**): 033302. DOI: 10.1088/1674-1056/21/3/033302

Nuclear dissociation after the O 1s $\rightarrow$ $(^4\Sigma_u^-)3s\sigma$ excitation in O_2 molecules

Bocheng Ding(丁伯承)[1,2,3], Ruichang Wu(吴睿昌)[1,2], Yunfei Feng(封云飞)[1,2], and Xiaojing Liu(刘小井)[1,2,†]

[1] *School Physical Science and Technology, ShanghaiTech University, Shanghai* 201210, *China*
[2] *Center for Transformative Science, ShanghaiTech University, Shanghai* 201210, *China*
[3] *University of Chinese Academy of Sciences, Beijing* 100049, *China*

(Received 26 December 2021; revised manuscript received 14 February 2022; accepted manuscript online 17 February 2022)

We investigate the dissociation dynamics of core-excited O_2 molecules using a high-resolution energy-resolved electron-ion coincidence experimental setup. The excited cationic states with two valence holes and one Rydberg electron are created after spectator Auger decay induced by O 1s $\rightarrow$ $(^4\Sigma_u^-)3s\sigma$ core excitation in O_2. From the energy correlation between the kinetic energy of the Auger electron and the ion kinetic energy release, we distinguish several dissociation channels. Rather complex dissociation channels of the spectator Auger final states are disclosed, which can be explained by the increased number of the crossing point due to the existence of Rydberg electron. The quantum system will evolve into different dissociation limits at each crossing point between the potential energy curves.

Keywords: nuclear dissociation, resonant excitation, spectator Auger

PACS: 33.80.Gj, 31.70.Hq, 32.80.Hd **DOI:** 10.1088/1674-1056/ac560b

1. Introduction

With the x-ray photon energy below the O 1s ionization threshold, the O_2 molecule can be promoted to an excited state, either bound or dissociative, triggering relaxation processes such as soft x-ray photon emission, resonant Auger electron emission, and deformation of molecular structure. If the excited state is bound, the molecule will mainly decay by emitting an electron, while the excited electron may participate in Auger decay or standby like a spectator.[1,2] If the excited state is highly dissociative, competition between molecular motion and electron emission will occur. In the extreme case, Auger decay can even happen after molecular dissociation.[3–7] As discussed here in the context of the O_2 molecules, Feifel *et al.*[8] investigated the participator Auger decay after O 1s $\rightarrow$ Rydberg excited O_2 with the photon energies across the *K*-shell resonance region. Tanaka *et al.*[9] comprehensively measured a series of resonant spectator Auger-electron spectra of O_2.

When an electron is excited to a Rydberg orbital, spectator Auger decay dominates the electronic decay processes and leaves the molecule to a two-hole-one-electron cationic state with two valence holes and one electron in a Rydberg orbital.[9,10] Because the Rydberg electron provides only partial screening of the repulsive force from the dicationic core, the two-hole-one-electron states are often dissociative.[11] Hikosaka *et al.*[12] found that most of the inner-valance-hole states of O_2^+ are strongly dissociative, and end up with a neutral atom and a singly charged ion. A rather comprehensive calculation of the potential energy curves was reported long time ago.[13] Using Doppler-free kinetic release spectroscopy and multireference configuration interaction calculations, the potential energy curves of O_2^{2+} were reported by Lundqvist *et al.*[14]

Compared with the singly and doubly ionized states, the dissociation of two-hole-one-electron states was much less investigated. Because either from an experimental point of view or from a theoretical point of view, the study of the two-hole-one-electron state is very difficult.[11] In our recent work, we measured the correlation between the Auger electrons and ions using a high-resolution energy-resolved coincidence experimental setup, after O 1sσ $\rightarrow$ $(^4\Sigma_u^-)4p\sigma$ excitation in O_2 molecules at the photon energy of 541.8 eV. We described that the O_2^+ two-hole-one-electron states dissociate into O^+ and O with a Rydberg electron, the results highlight how the spectator Rydberg electron participates in the dissociation of the Auger final states.[15] We also found that some weak channels correspond to dissociated O^+ and O without a Rydberg electron after time-consuming fine-tuning of parameters in data analysis, which points toward selectivity on the orbital size in the dissociation processes of the spectator Auger final states.[11] In this paper, we switch the measurement and analysis at the photon energy of 538.95 eV, which corresponds to O 1sσ $\rightarrow$ $(^4\Sigma_u^-)3s\sigma$ core excitation in O_2.

2. Experimental method

Since the experimental method has already been described in detail in Refs. [11,15], only a brief description is given here. The experiments were carried out using the EPICEA setup at the PLEIADES beamline[16] at synchrotron

†Corresponding author. E-mail: liuxj@shanghaitech.edu.cn
© 2022 Chinese Physical Society and IOP Publishing Ltd

SOLEIL in Saint-Aubin, France. This setup is specially designed for high kinetic-energy electron-ion coincidence measurement, which is composed of a double-toroidal electron analyzer (DTA)[17,18] and an ion TOF spectrometer.

The DTA selected the electron with an emission direction in the polar angle of 54±3° with respect to its symmetry axis and the azimuthal angles from 0° to 360°. The photon energy was set as 538.95 eV, which corresponds to O $1s\sigma \rightarrow (^4\Sigma_u^-)3s\sigma$ core excitation in O_2,[9] and the light polarization was parallel to the symmetry axis of the setup. The DTA was operated with the pass energy of 80 eV, the central kinetic energy was set at 509 eV, and the electron energy resolution was about 0.7 eV. Opposite to the DTA, there is an ion TOF spectrometer incorporating 3D focusing mode. A pulsed ±100 V ion extraction field (15 mm spacing) was triggered upon the detection of an Auger electron and pushed the ions toward the ion detector. The mass resolution of the nearly zero kinetic energy ions is about 1000, the ion momentum resolution is about 1.2–1.6 a.u., and the ion energy resolution was ∼0.3 eV. A random signal generator was used to simulate the false coincident event, and their contribution was subtracted according to the method described by Prümper *et al.*[19]

3. Result and discussion

The resonant Auger electron energy spectrum following O $1s\sigma \rightarrow (^4\Sigma_u^-)3s\sigma$ excitation in O_2 at the photon energy of 538.95 eV is shown in Fig. 1, which covers the kinetic-energy range from 504 eV to 514 eV (corresponding to a binding energy range from 24.95 eV to 34.95 eV). Peaks above 507 eV are much broader than the peaks below. Because the former peaks come from O_2 $(1s^{-1}\sigma^*)$ state, whose potential energy curve is highly dissociative and covers a broad energy range within the Franck–Condon region.[4] In contrast, the later peaks come from $O_2(1s^{-1}{}^4\Sigma_u^-)3s\sigma$ bound state, so widths of these peaks are much narrower. To our knowledge, the assignments of the former peaks have not been reported in literature, while the assignments of the latter are adopted from Tanaka *et al.*[9]

The ion time-of-flight spectrum is shown in Fig. 2. The peak of O_2^+ is very narrow because its kinetic energy can only be contributed by the thermal motion and the recoil during electron emission. The profile of O^+ is very broad and splits into two wings, because O $1s\sigma \rightarrow (^4\Sigma_u^-)3s\sigma$ Rydberg excitation is sitting on the top of O $1s \rightarrow \sigma^*$ resonance,[6] which occurs preferentially when the molecular axis is parallel to the polarization vector of the incoming photons and the axis of TOF spectrometer, and the molecular orientation is preserved during molecular fragmentation, which is generally faster than molecular rotation in this case. We cannot present here the electron spectrum related to O_2^+ due to very low statistics.

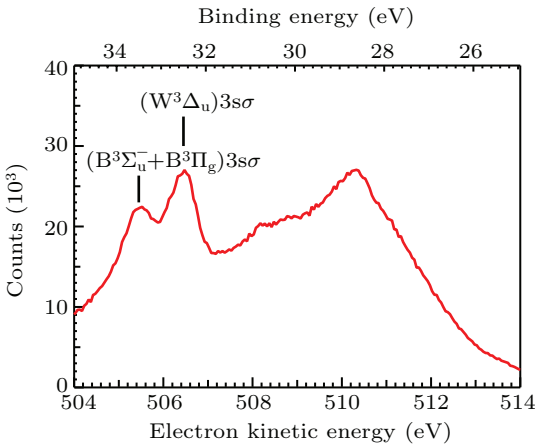


Fig. 1. The resonant Auger electron spectrum after O $1s\sigma \rightarrow (^4\Sigma_u^-)3s\sigma$ excitation in O_2 at the photon energy of 538.95 eV. Assignments of two spectator Auger final states are adopted from Tanaka *et al.*[9]

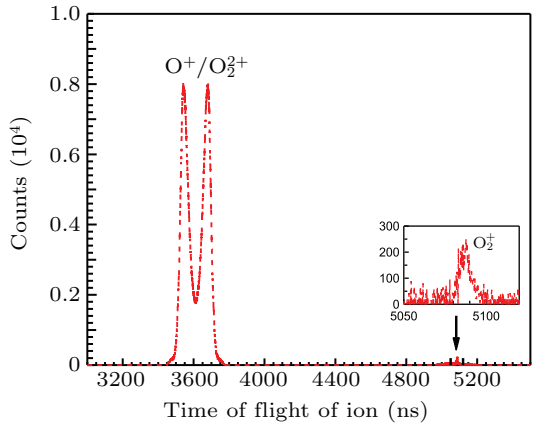


Fig. 2. Ion time-of-flight spectrum recorded after O $1s\sigma \rightarrow (^4\Sigma_u^-)3s\sigma$ excitation in O_2 at the photon energy of 538.95 eV. The inset shows a magnified O_2^+ peak.

Under the assumption that the kinetic energy of the neutral atom equals that of the ion, we plot the ion kinetic energy release (KER: the sum of the kinetic energies of all fragments) against the Auger electron kinetic energy in Fig. 3. These features are located above the blue dashed tilted line, which represent the appearance threshold of $O^+ + O^+$, so the reaction processes can be described as $O_2(1s^{-1}{}^4\Sigma_u^-)3s\sigma \rightarrow O^+ + O + e^-_{Auger}$. These features can be grouped by tilted lines with the slope of −1 due to the energy conservation law in the decay processes:

$$\begin{aligned} E(h\nu) &= E_k(e^-_{Auger}) + E_{KER} + E_i(O) \\ &\quad + E_i(O^+) + E_{IP}(O) + E_D(O_2). \end{aligned} \tag{1}$$

Here $E(h\nu)$ is the photon energy, $E_k(e^-_{Auger})$ is the Auger electron kinetic energy, E_{KER} is the kinetic energy release of fragments in the dissociation processes, $E_i(O)$ and $E_i(O^+)$ are the excitation energies of the atom and ion, respectively, $E_{IP}(O)$ is the ionization potential of the oxygen atom, and $E_D(O_2)$ is the dissociation energy of O_2 molecule at the ground state. The dissociation limit energy E_{diss} is defined as

$$\begin{aligned} E_{diss} &= E(h\nu) - E_k(e^-_{Auger}) - E_{KER} \\ &= E_i(O) + E_i(O^+) + E_{IP}(O) + E_D(O_2). \end{aligned} \tag{2}$$

The dissociation limits energies $E_{\rm diss}$ are calculated using Eq. (1) and assigned using Eq. (2) with the energy values from the NIST atomic database,[20] as listed in Table 1. The various $E_{\rm diss}$'s are represented by the red dashed tilted lines in Fig. 3. Here, we label them as I, II, III, and IV. In Table 1, we also list the other dissociation limits which do not show observable intensities, as indicated by circles in Table 1 and by four green dashed tilted lines in Fig. 3.

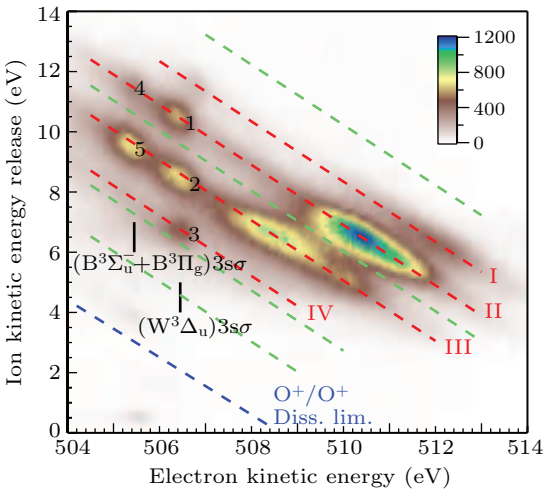


Fig. 3. The correlation between the kinetic energy release of the fragments and the kinetic energy of the Auger electron at the photon energy of 538.95 eV. The red dashed tilted lines I, II, III, and IV represent groups of dissociation limits after spectator Auger decay. The green dashed tilted lines indicate the missing dissociate limits. The blue dashed tilted line indicates the appearance threshold of $O^+ + O^+$. The assignments of spectator Auger lines are adopted from Tanaka *et al.*[9]

Table 1. Assignment of the dissociation limit energy $E_{\rm diss}$ for the features observed in Fig. 3. Symbols ◯ are used to mark missing features in Fig. 3. The unit of energy is eV.

O	$(O^+)^4S$		$(O^+)^2D$		$(O^+)^2P$	
	$E_{\rm diss}$	Label	$E_{\rm diss}$	Label	$E_{\rm diss}$	Label
^3P	18.72	◯	22.04	II	23.74	III
^1D	20.69	I	24.01	III	25.71	IV
^1S	22.91	◯	26.23	◯	27.93	◯

As indicated by green dashed tilted lines in Fig. 3, it can be seen that the first, fourth, seventh, and eighth limits do not show observable intensities. This puzzle can be explained by examining a comprehensive summary of potential curves of O_2^+ calculated by Beede *et al.*[13] Among them, we choose repulsive potential curves with proper symmetry, correct binding energy in the Franck–Condon region, and dissociate into the limits given in Table 1. We find that the $^{2,4}\Delta_u$, the $^{2,4}\Sigma_u^-$, and the $^{2,4}\Pi_g$ from Beede *et al.*[13] are the candidates. As a result, only the second, third, fifth, and sixth limits should exist, which agrees reasonably well with the observed I, II, III, and IV limits in Table 1.

The dissociation of the highly excited diatomic molecules can be very complicated. For example, the dissociation of super-excited F_2 molecule into F^+/F^- pair was calculated by Zhang *et al.*[21] In our recent paper, rather complex dissociation channels of the two-hole-one-electron Auger final states are observed,[15] which also appear in this work. As reported by Lundqvist *et al.*,[14] there are three dissociation channels for O_2^{2+}:

$$\begin{aligned} O_2^{2+}(W^3\Delta_u) &\rightarrow O^+(^4S)+O^+(^2D),\\ O_2^{2+}(B'^3\Sigma_u^-) &\rightarrow O^+(^4S)+O^+(^2D),\\ O_2^{2+}(B^3\Pi_g) &\rightarrow O^+(^4S)+O^+(^4S). \end{aligned}$$

Here, $O^+(^2P)$ cannot be created if we assume that the Rydberg electron acts purely as a spectator of the dissociation of the dicationic core O_2^{2+}. However, the appearance of the dissociation limit III and IV proves that Rydberg electrons are not acting purely as a spectator. It is can be expected that, compared with dicationic ion, the spectator Auger final state with an excited Rydberg electron would pass more potential curve cross points before dissociation is accomplished.[15] Therefore, more dissociation limits are expected.

From Fig. 3, it might be puzzling that the $(W^3\Delta_u)3s\sigma$ state dissociates into more channels than the $(B'^3\Sigma_u^- + B^3\Pi_g)3s\sigma$ state. To facilitate the discussion, the dissociation channels are numbered from 1 to 5 in Fig. 3, 1 to 3 result from the $(W^3\Delta_u)3s\sigma$ state, while channels 4 and 5 from the $(B'^3\Sigma_u^- + B^3\Pi_g)3s\sigma$ state. We compared our measurements with the probable candidates reported by Beede *et al.*[13] in Table 2. For the $(W^3\Delta_u)3s\sigma$ state, three limits II, III, IV are reached. However, the $(B'^3\Sigma_u^- + B^3\Pi_g)3s\sigma$ state was predicted to lead to dissociation limits I, II, and III, but only II and III were observed here. Therefore, the $(W^3\Delta_u)3s\sigma$ state can observe more dissociation channels. From another point of view, the observed features grouped by the limit II, III, and IV are well explained by comparison with the calculation of Beede *et al.*, except for the limit I from $^{2,4}\Pi_g$ state. Considering Beede *et al.* made the calculation several decades ago, we suggest updating the calculation by theoretical in the future.

Table 2. Assignment of the dissociation channels after O $1s\sigma \rightarrow (^4\Sigma_u^-)3s\sigma$ excitation in O_2. Number and ◯ symbols are used to mark observable and missing features in our measurements, respectively. Based on the potential curves reported by Beede *et al.*, √ and × symbols are used to indicate the feature should exist and not, respectively.

	Measurements		Beede *et al.*		
	$(W^3\Delta_u)3s\sigma$	$(B'^3\Sigma_u^- + B^3\Pi_g)3s\sigma$	$^{2,4}\Delta_u$	$^{2,4}\Sigma_u^-$	$^{2,4}\Pi_g$
I	◯	◯	×	×	√
II	1	4	√	×	√
III	2	5	√	√	√
IV	3	◯	√	×	×

4. Conclusions

With the help of the energy-resolved Auger electron-ion coincidence technique, we have investigated the dissociation processes of the spectator Auger final states after the O $1s\sigma \rightarrow (^4\Sigma_u^-)3s\sigma$ excitation in O_2 molecules. The spectator Auger final states dissociate into O^+ and O without a Rydberg electron, we are able to distinguish different dissociation channels from the correlation between the electron kinetic energy and the ion kinetic energy. Compared with the dissociation processes of dicationic states O_2^{2+}, rather complex dissociation channels of the spectator Auger final states are disclosed. It is expected that a spectator Auger final state with an excited Rydberg electron would pass more potential curve cross points than the dicationic state. As a result, more dissociation limits are reached.

Acknowledgements

Project supported by the National Natural Science Foundation of China (Grant No. 11574020), the Project of Thousand Youth Talents in China, and the Starting Grant of ShanghaiTech University.

References

[1] Gel'mukhanov F and Ågren H 1999 *Phys. Rep.* **312** 87
[2] Piancastelli M N 2000 *J. Electron Spectrosc. Relat. Phenom.* **107** 1
[3] Morin P and Nenner I 1986 *Phys. Rev. Lett.* **56** 1913
[4] Björneholm O, Sundin S, Svensson S, Marinho R R T, Naves de Brito A, Gel'mukhanov F and Ågren H 1997 *Phys. Rev. Lett.* **79** 3150
[5] Pahl E, Cederbaum L S, Meyer H D and Tarantelli F 1998 *Phys. Rev. Lett.* **80** 1865
[6] Björneholm O, Bässler M, Ausmees A, Hjelte I, Feifel R, Wang H, Miron C, Piancastelli M N, Svensson S, Sorensen S L, Gel'mukhanov F and Ågren H 2000 *Phys. Rev. Lett.* **84** 2826
[7] Liu X J, Miao Q, Gel'mukhanov F, Patanen M, Travnikova O, Nicolas C, Ågren H, Ueda K and Miron C 2015 *Nat. Photon.* **9** 120
[8] Feifel R, Tanaka T, Kitajima M, Tanaka H, De Fanis A, Sankari R, Karlsson L, Sorensen S, Piancastelli M N, Prümper G, Hergenhahn U and Ueda K 2007 *J. Chem. Phys.* **126** 174304
[9] Tanaka T, Feifel R, Kitajima M, Tanaka H, Sorensen S L, Sankari R, De Fanis A, Piancastelli M N, Karlsson L and Ueda K 2008 *Phys. Rev. A* **78** 022516
[10] Gejo T, Oura M, Tokushima T, Horikawa Y, Arai H, Shin S, Kimberg V and Kosugi N 2017 *J. Chem. Phys.* **147** 044310
[11] Tian L, Ding B, Nicolas C, Wu R, Feng Y, Patanen M, Nandi S, Bozek J, Miron C and Liu X J 2021 *Phys. Rev. A* **103** 043103
[12] Hikosaka Y, Aoto T, Hall R I, Ito K, Hirayama R, Yamamoto N and Miyoshi E 2003 *J. Chem. Phys.* **119** 7693
[13] Beebe N H F, Thulstrup E W and Andersen A 1976 *J. Chem. Phys.* **64** 2080
[14] Lundqvist M, Edvardsson D, Baltzer P, Larsson M and Wannberg B 1996 *J. Phys. B: At. Mol. Opt. Phys.* **29** 499
[15] Song S, Ding B, Xu W, Nicolas C, Patanen M, Nandi S, Bozek J, Miron C, Xiao Z and Liu X J 2019 *Phys. Rev. A* **99** 022511
[16] Miron C and Morin P 2009 *Nucl. Instrum. Methods Phys. Res. Sect. A* **601** 66
[17] Miron C, Simon M, Leclercq N and Morin P 1997 *Rev. Sci. Instrum.* **68** 3728
[18] Le Guen K, Céolin D, Guillemin R, Miron C, Leclercq N, Bougeard M, Simon M, Morin P, Mocellin A, Burmeister F, Naves de Brito A and Sorensen S L 2002 *Rev. Sci. Instrum.* **73** 3885
[19] Prümper G and Ueda K 2007 *Nucl. Instrum. Methods Phys. Res. Sect. A* **574** 350
[20] Atomic Spectra Database 2016 *physics.nist.gov/asd/*
[21] Zhang W H, He C L, Hao Y S, MO Y X and Li J M 2007 *Chin. Phys. Lett.* **24** 1220